Supporting Information

Formation and Physicochemical Characteristics of Nano Biochar: Insight into Chemical and Colloidal Stability

Guocheng Liu,[†] Hao Zheng,[‡] Zhixiang Jiang,[§] Jian Zhao,[‡] Zhenyu Wang,[*,†] Bo Pan,[‖] and Baoshan Xing[*,⊥]

[†] *Institute of Environmental Processes and Pollution Control, and School of Environmental and Civil Engineering, Jiangnan University, Wuxi 214122, China*

[‡] *College of Environmental Science and Engineering, and Key Laboratory of Marine Environment and Ecology, Ministry of Education, Ocean University of China, Qingdao 266100, China*

[§] *College of Environmental Science and Engineering, Qingdao University, Qingdao 266071, China*

[‖] *Faculty of Environmental Science and Engineering, Kunming University of Science and Technology, Kunming 650500, China*

[⊥] *Stockbridge School of Agriculture, University of Massachusetts, Amherst, MA 01003, Massachusetts 01003, United States*

Corresponding author:

*B.S. Xing, Phone: +1 413 545 5212. E-mail: bx@umass.edu.

*Z.Y. Wang, Phone: +86 510 85911123. E-mail: wang0628@jiangnan.edu.cn.

Name of the journal: *Environmental Science & Technology*

Date of the document prepared: August 24, 2018

Pages: 31

Figures: 22

Tables: 4

Correction of OD_{800} and yield of nano biochars. The ultrafiltrates of low-temperature biochar (BC) (300 °C) extraction were light-colored (Figure S1A), suggesting that the suspensions of nano biochars (N-BCs) contained non-negligible amount of dissolved organic carbon (DOC). The DOC fraction in BCs has been often reported in many studies.[1,2] Therefore, OD_{800} values of N-BC extractions were adjusted by deducting the OD_{800} values of their ultrafiltrates from those of the unfiltered suspensions. The ultrafiltrates were obtained using a 15-mL Millipore centrifuge tube with ~3 nm membrane (3-nm tube, Germany) to centrifuge the N-BC suspensions at 4000 rpm for 15 min. Yields of residual and colloidal BCs (R-BCs and C-BCs) were calculated using a ratio of their mass measured by a highly precise balance (readability 0.01 mg) to that of bulk BCs (B-BCs). For the different temperature N-BCs, the OD800 values of their suspensions cannot accurately represent their yields due to the differences in transmittance and reflectance properties (Figure S4). Meanwhile, no maximum absorption peak of N-BCs was observed by the UV-Vis analyses (Lambda 35, PerkinElmer, USA) (Figure S1D). Thus, the yields of N-BCs ($Yield_{N\text{-}BC}$, %) were calculated based on the total C concentration of the suspensions ($C_{suspension}$, mg C/L) and the ultrafiltrates ($C_{ultrafiltrate}$, mg C/L) determined by a TOC analyzer (TOC-VCSN, Shimadzu, Japan) and their C content ($C_{N\text{-}BC}$, %) measured with an elemental analyzer (MicroCube, Elementar, Germany), presented as follows:

$$Yield_{N\text{-}BC}=(C_{suspension}-C_{ultrafiltrate})\times V/C_{N\text{-}BC}/M_{B\text{-}BC}\times 100\%$$

where V is suspension volume (L) and $M_{B\text{-}BC}$ is weight of B-BCs (mg).

Preparation of residual, colloidal and nano biochar powders. Bulk peanut shell BC

(B-PBC) (75–150 μm, 8 g) and 400 mL deionized water (DI) were both placed into a 500-mL glass beaker, and sonicated at 700 W (FB705, Fisher Scientific, USA) at 25 °C using cooling water for 10 min. The suspension was immediately sub-packed in 40-mL vials carefully, and underwent the extraction procedure for N-BCs, and then freeze-dried at –50 °C using a FD5-series vacuum freeze dryer (SIM, USA) for R-PBC, C-PBC, and N-PBC powders, respectively. Before freeze-drying, R-PBCs and C-PBCs were rinsed with DI for four times, respectively, and the suspensions of N-PBCs were concentrated using 3-nm tube and washed by DI repeatedly.

Characterization of biochars. Total C, H, N, and O content of BC samples were obtained by elemental analyzer, and atomic ratios of H/C, O/C, and (O+N)/C were calculated. The BC pH was determined in DI (1:20 w/v) stirred at 150 rpm for 24 h (AB15, Fisher Scientific, USA). Ash content was measured by burning the samples in a muffle furnace at 750 °C for 6 h. Surface area of BCs was analyzed based on N_2 adsorption-desorption isotherm at 77 K using an Autosorb-1 (Quantachrome, USA).

Scanning electron microscopy (SEM, S4800, Hitachi, Japan), transmission electron microscopy (TEM, H-7650, Hitachi, Japan) and atomic force microscopy (AFM, 5400, Agilent, USA) were employed to investigate morphology properties of the BCs. For SEM, the powders of B-PBCs and R-PBCs were directly adhered to a double coated carbon conductive tape, and 50-μL suspension of C-PBCs was dropped onto the aluminum foil (1 cm × 1 cm), whose reverse side was adhered onto the carbon conductive tape, and then deposited and air-dried. For TEM, the suspension of N-PBCs was properly diluted, and one drop (~10 μL) was deposited on the copper grid with

lacey carbon support, and then air-dried for 24 h. The values of diameter (lateral size) and thickness (height profile) of N-PBCs were examined by AFM.

The BCs were subjected to Fourier transform infrared spectroscopy (FTIR, Tensor 27, Bruker Optics, Germany), X-ray photoelectron spectroscopy (XPS, ESCALAB 250Xi, Thermo scientific, USA), Raman (DXR Raman Microscope, Thermo Scientific, USA), and X-ray diffractometer (XRD, D8 Advance, Bruker, Germany). FTIR spectra of the samples were recorded in a range of 400-4000 cm^{-1} with a resolution of 2 cm^{-1}. Surface elemental compositions and chemical states of the BCs were measured by XPS, and XPS-peak-differentiation-imitating analysis was operated using a Gaussian-Lorentzian curve-fitting program (XPSPEAK 4.1). Raman spectra were collected with the range from 100 to 3500 cm^{-1}. XRD was carried out at 35 kV, 25 mA in the range between 5 ° to 60 ° with a step size of 0.02 °, and XRD pattern was analyzed by Jade 5.0 (Material Data, Inc.).

Table S1. Characteristics of biochar, graphite, and activated carbon samples.

Samples [α]	Elemental content [β] (%)				Atomic ratio			pH	Ash (%)	ID/IG [γ]
	C	H	O	N	H/C	O/C	(O+N)/C			
B-FBC300	75.8	6.58	14.8	2.31	1.04	0.15	0.17	7.16±0.10d[δ]	14.0±0.3d	0.69±0.04a
B-FBC400	76.0	5.64	13.9	2.33	0.89	0.14	0.16	8.19±0.03c	16.9±0.8c	0.68±0.01a
B-FBC500	79.1	4.58	10.5	2.49	0.69	0.10	0.13	9.28±0.11b	21.1±0.4a	0.64±0.01ab
B-FBC600	80.0	3.81	9.26	2.38	0.57	0.09	0.11	10.1±0.01a	19.9±0.6b	0.61±0.01b
B-CBC300	56.7	3.93	24.2	1.36	0.83	0.32	0.34	6.40±0.04d	13.1±0.1c	0.85±0.01a
B-CBC400	60.3	3.26	19.9	1.14	0.65	0.25	0.26	7.47±0.07c	13.5±0.2c	0.79±0.06ab
B-CBC500	67.2	2.54	13.4	1.02	0.45	0.15	0.16	8.95±0.09b	14.3±0.2b	0.77±0.00b
B-CBC600	67.2	1.88	10.9	0.87	0.34	0.12	0.13	9.58±0.05a	15.3±0.4a	0.73±0.04b
B-MBC300	60.1	4.42	19.9	3.37	0.88	0.25	0.30	6.87±0.06d	12.4±0.4c	0.89±0.02a
B-MBC400	61.0	3.63	17.5	3.27	0.71	0.22	0.26	7.25±0.07c	19.0±0.8b	0.79±0.01b
B-MBC500	65.7	2.72	12.8	2.92	0.50	0.15	0.18	9.16±0.11b	19.4±1.0b	0.76±0.00b
B-MBC600	68.7	2.08	11.0	2.37	0.36	0.12	0.15	9.53±0.05a	20.4±0.5a	0.75±0.00b
Graphite	96.7	0.25	2.36	0.05	0.03	0.02	0.02	6.22±0.03* [ε]	ND [ζ]	0.19±0.01
N-G	90.3	0.55	4.31	2.96	0.07	0.04	0.06	4.49±0.11		0.32±0.03*
CAC	55.9	3.26	18.7	0.57	0.70	0.25	0.26	7.88±0.04*		0.69±0.07
CHAC	60.2	3.26	19.8	1.16	0.65	0.25	0.26	6.70±0.10		0.78±0.04

[α] B-FBC*X*, B-CBC*X*, and B-MBC*X* are the bulk biochars prepared from furfural residues, cotton straw, and Chinese medicine residues, respectively, where *X* represents pyrolytic temperature. N-G, CAC, and CHAC are nano graphite, coaly activated carbon, and coconut husk activated carbon, respectively. The natural graphite, CAC, and CHAC were provided by Sinopharm group Co. Ltd, China, and N-G was purchased from Nanjing XFNANO Materials Tech Co., Ltd, China.

[β] Elemental composition of the samples was measured by elemental analyzer.

[γ] ID/IG is the intensity ratio of D band to G band of the samples by raman analysis.

[δ] The different letters behind the data indicate significant differences among the BCs from the same feedstock at different temperatures ($n = 3$, $p < 0.05$).

[ε] The asterisk represents significant difference between the natural graphite and N-G ($n = 3$, $p < 0.05$).

[ζ] ND represents the data are not determined.

Table S2. Surface elemental composition and atomic ratio of biochar, graphite, and activated carbon samples by XPS.

Samples [α]	Elemental content %						Atomic ratio	
	C	O	N	S	Si	Al	O/C	(O+N)/C
B-PBC300	72.9	16.0	2.61	0.97	5.73	1.76	0.165	0.196
R-PBC300	74.5	15.7	2.45	0.64	6.28	0.42	0.158	0.186
C-PBC300	71.0	18.5	2.81	0.53	5.13	2.11	0.195	0.229
N-PBC300	62.2	25.9	2.13	0.56	6.56	2.70	0.312	0.341
B-PBC400	72.8	16.7	2.82	0.41	6.62	0.64	0.172	0.205
R-PBC400	77.8	13.1	2.36	0.62	5.60	0.54	0.126	0.152
C-PBC400	73.2	16.0	2.04	0.59	6.84	1.30	0.164	0.188
N-PBC400	70.0	19.7	2.01	0.50	6.84	0.92	0.211	0.236
B-PBC500	74.1	14.6	2.64	0.56	6.55	1.63	0.147	0.178
R-PBC500	79.5	11.6	2.71	0.51	5.07	0.62	0.110	0.139
C-PBC500	72.8	16.2	2.44	0.42	6.47	1.72	0.167	0.196
N-PBC500	72.4	16.7	2.32	0.57	5.56	2.53	0.173	0.200
B-PBC600	81.5	10.4	1.74	0.47	4.72	1.20	0.095	0.114
R-PBC600	82.5	10.0	1.36	0.42	4.83	0.87	0.091	0.105
C-PBC600	80.9	10.4	1.90	0.39	5.06	1.32	0.097	0.117
N-PBC600	79.3	11.0	1.86	0.47	5.10	2.24	0.104	0.124
Graphite	95.2	2.53	0.17	0.17	0.87	1.05	0.020	0.022
N-G	90.7	6.27	0.96	0.38	0.97	0.70	0.052	0.061
CAC	60.9	19.9	2.22	0.89	11.5	4.57	0.245	0.277
CHAC	74.2	16.3	2.70	0.76	4.97	1.13	0.165	0.196

[α] B-PBC*X*, R-PBC*X*, C-PBC*X*, and N-PBC*X* are the bulk, residual, colloidal, and nano peanut shell-derived biochars, respectively, where *X* represents pyrolytic temperature. N-G, CAC, and CHAC are the nano graphite, coaly activated carbon, and coconut husk activated carbon, respectively.

Table S3. Surface composition of C functional groups of the biochar fractions by XPS.

Samples	Functional groups (% of total C)			
	C=C/C–C/C–H	C–O	C=O	O=C–O
B-PBC300	48.7±0.44	26.4±0.59	14.4±0.40	10.5±0.25
R-PBC300	55.8±0.17	28.8±0.47	10.5±0.21	4.91±0.10
C-PBC300	46.4±0.13	30.9±0.08	13.0±0.03	9.78±0.24
N-PBC300	41.6±0.27	30.6±0.26	15.5±0.46	12.3±0.45
B-PBC600	75.0±0.21	13.9±0.52	ND	11.0±0.73
R-PBC600	81.1±0.33	12.1±0.14		6.81±0.18
C-PBC600	76.2±0.38	13.6±0.13		10.2±0.51
N-PBC600	73.4±0.43	17.7±0.35		8.90±0.08

ND represents data that were not detected.

Table S4. Physicochemical properties and cation concentration of the natural waters.

Water samples	pH	DOC[α] mg C/L	EC[β] μS/cm	Cations (mg/L)			
				K^+	Na^+	Ca^{2+}	Mg^{2+}
Lake	7.13 ± 0.06	10.7 ± 1.06	930 ± 17.2	3.44	82.9	67.5	19.6
River	7.36 ± 0.08	17.5 ± 1.27	433 ± 9.17	8.03	30.4	30.0	8.96
Spring	6.39 ± 0.12	8.04 ± 0.21	3.57 ± 0.12	1.38	0.82	20.7	6.87

[α] DOC is dissolved organic carbon.

[β] EC is electric conductivity.

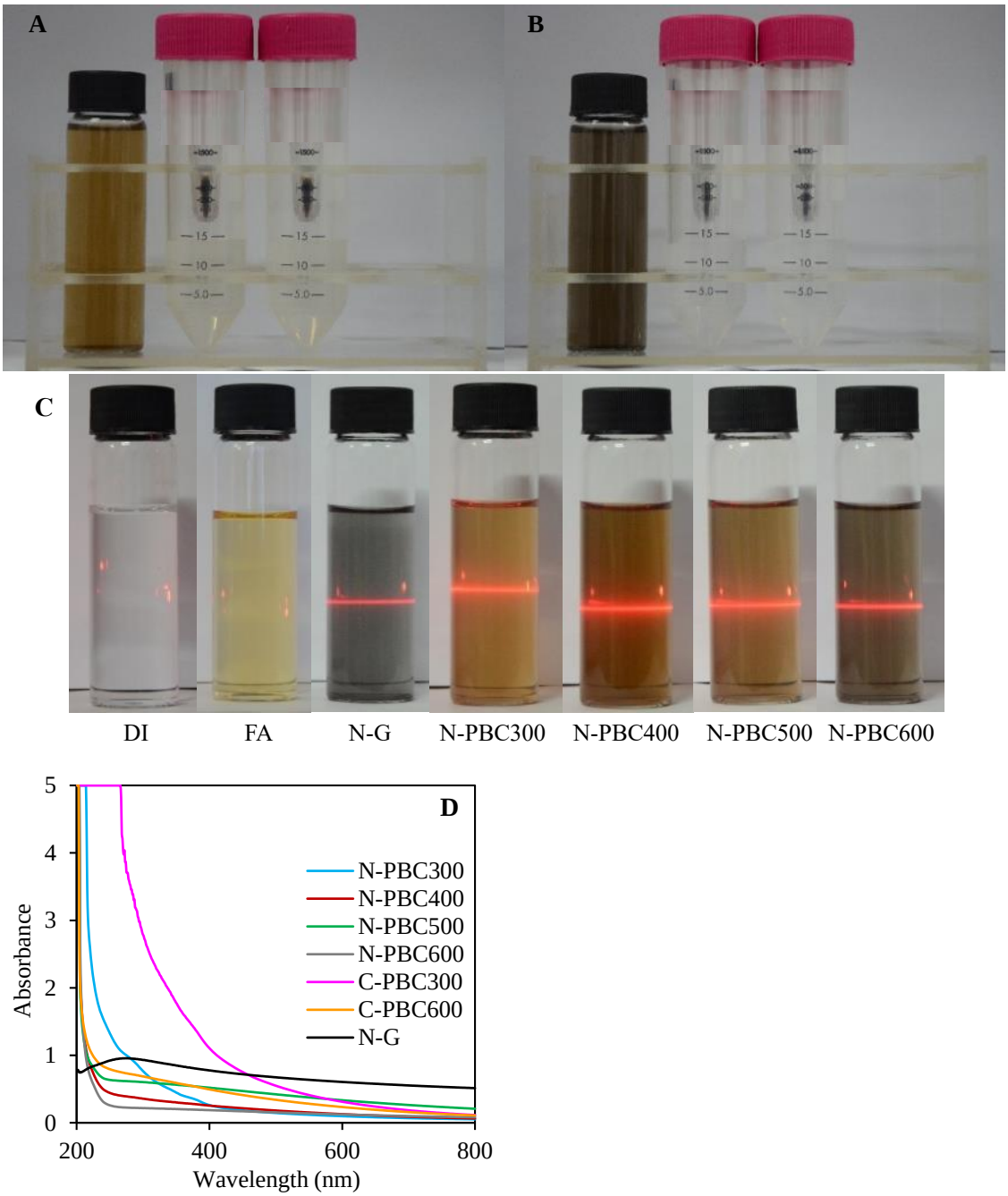

Figure S1. Photographs of (A) N-PBC300 and (B) N-PBC600 suspensions before and after ultrafiltration. (C) Tyndall effect of deionized water (DI), fulvic acid (FA), nano graphite (N-G), and N-PBCs. (D) UV-Vis absorbance of N-PBC suspensions. The Suwannee River FA was provided by International Humic Substances Society (IHSS).

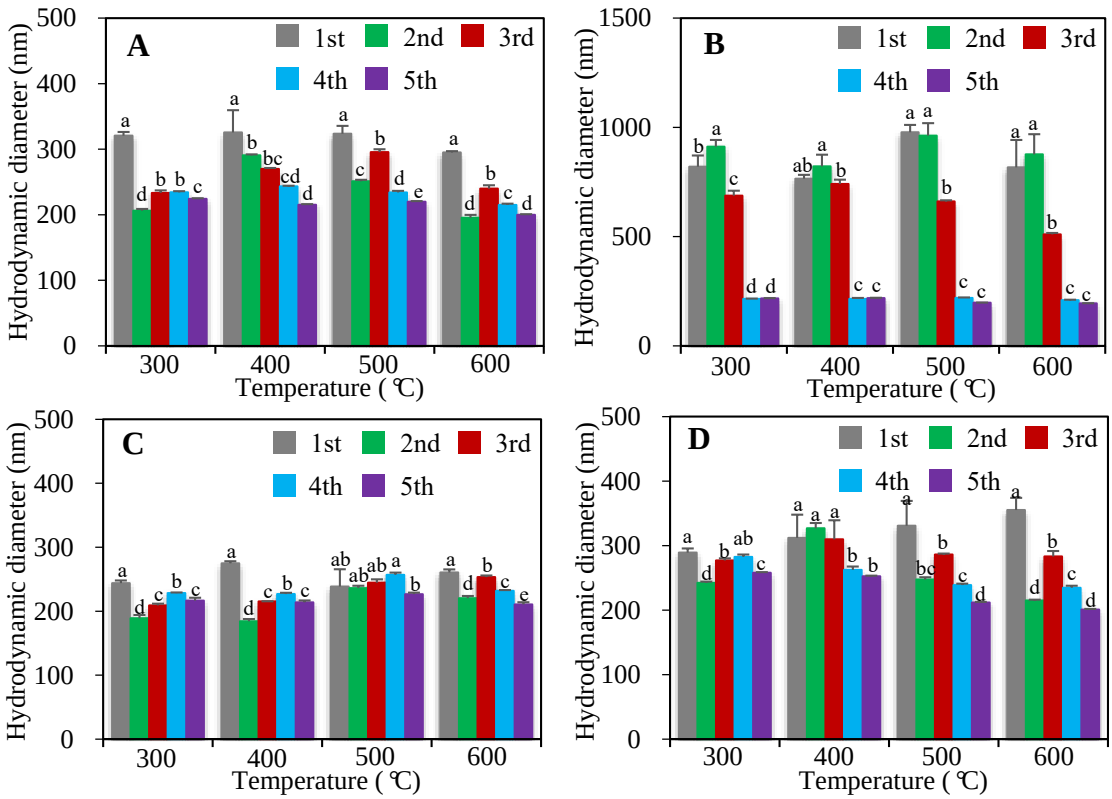

Figure S2. Hydrodynamic diameter of the nano biochars (N-BCs) from bulk biochars (B-BCs) of (A) peanut shell, (B) furfural residues, (C) cotton straw, and (D) Chinese medicine residues during the five consecutive extraction processes. For a given temperature, the different letters indicate significant difference in hydrodynamic diameter among N-BCs in the five consecutive extraction processes. Little release of N-BCs from B-FBCs in the initial three extraction treatments (Figure S3A and S5B below) would be responsible for the abnormally high hydrodynamic diameter in panel (B).

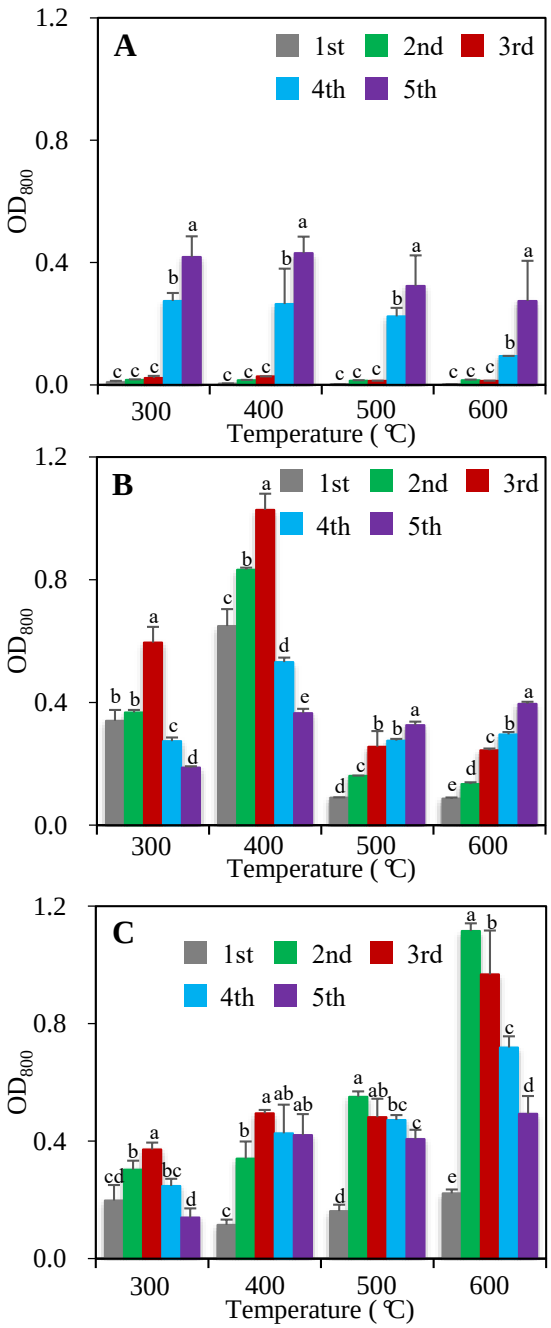

Figure S3. Release of the nano biochars (N-BCs) from bulk biochars (B-BCs) of (A) furfural residues, (B) cotton straw, and (C) Chinese medicine residues in the five consecutive extractions. For a given temperature, the different letters indicate significant difference among the N-BC release during the five consecutive extraction processes.

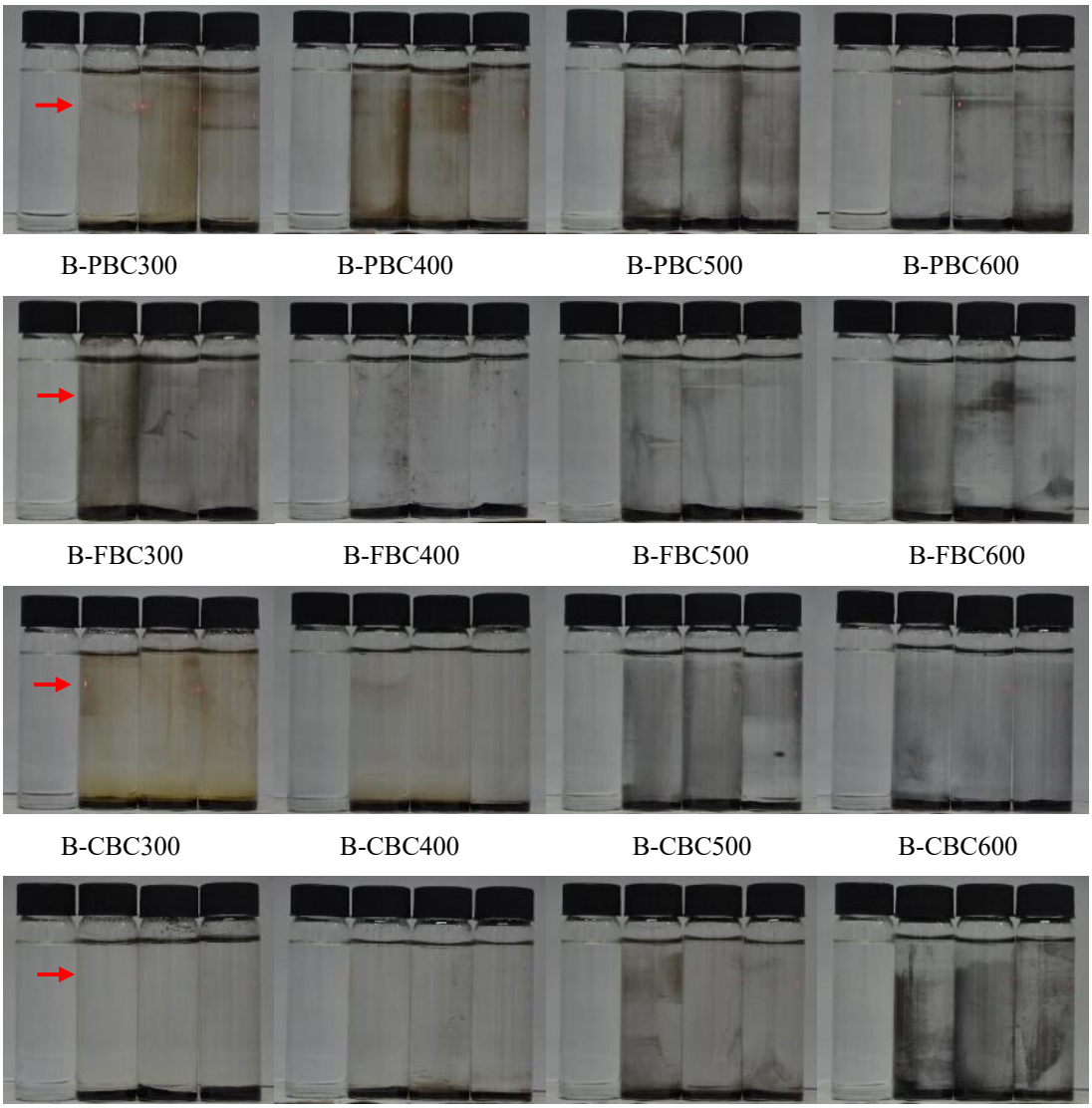

Figure S4. Images of bulk biochars (B-BCs) after the fractionation process for the nano biochars (N-BCs) without the sonication treatment. Unobvious Tyndall effect (red arrows, illuminant position) suggested that little N-BCs were released from B-BCs in the non-sonication treatment.

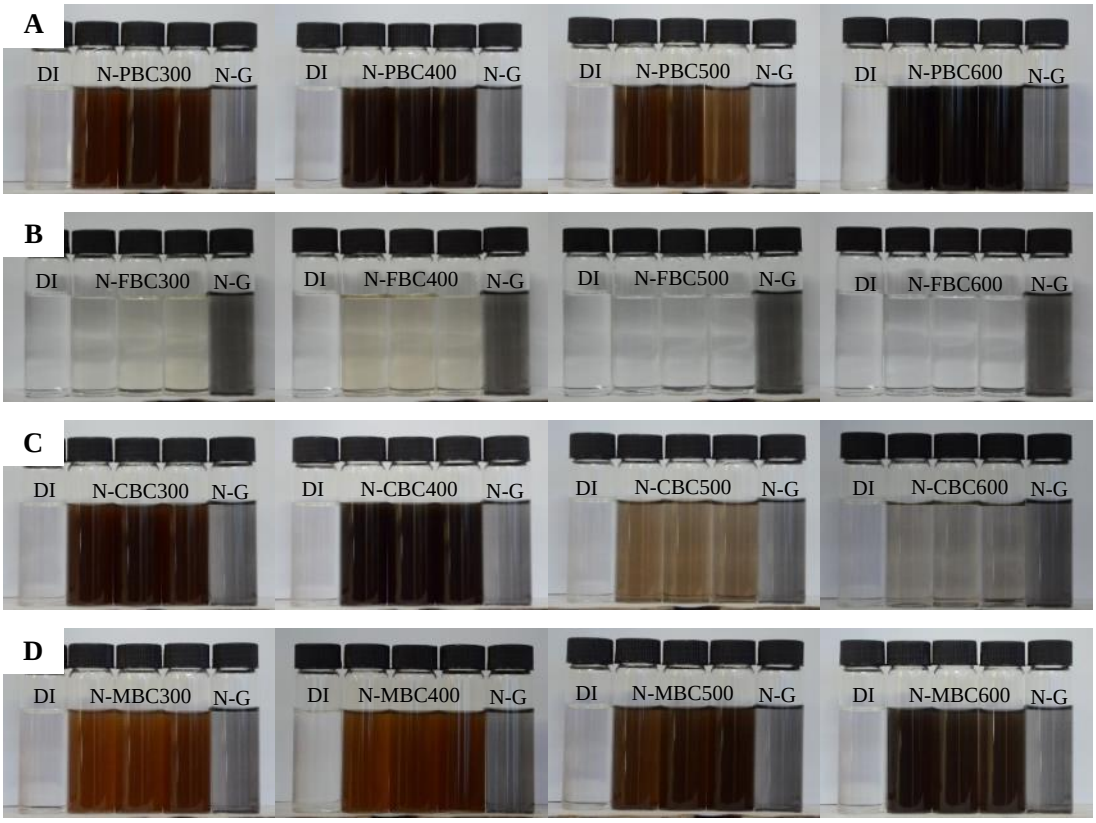

Figure S5. The suspensions of nano biochars (N-BCs) from bulk biochars (B-BCs) in the third extraction. N-PBC*X*, N-FBC*X*, N-CBC*X*, and N-MBC*X* are the N-BCs from the B-BCs prepared of peanut shell, furfural residues, cotton straw, and Chinese medicine residues, respectively, where *X* represents pyrolytic temperature. Deionized water (DI) and nano graphite (N-G) suspension were employed as control.

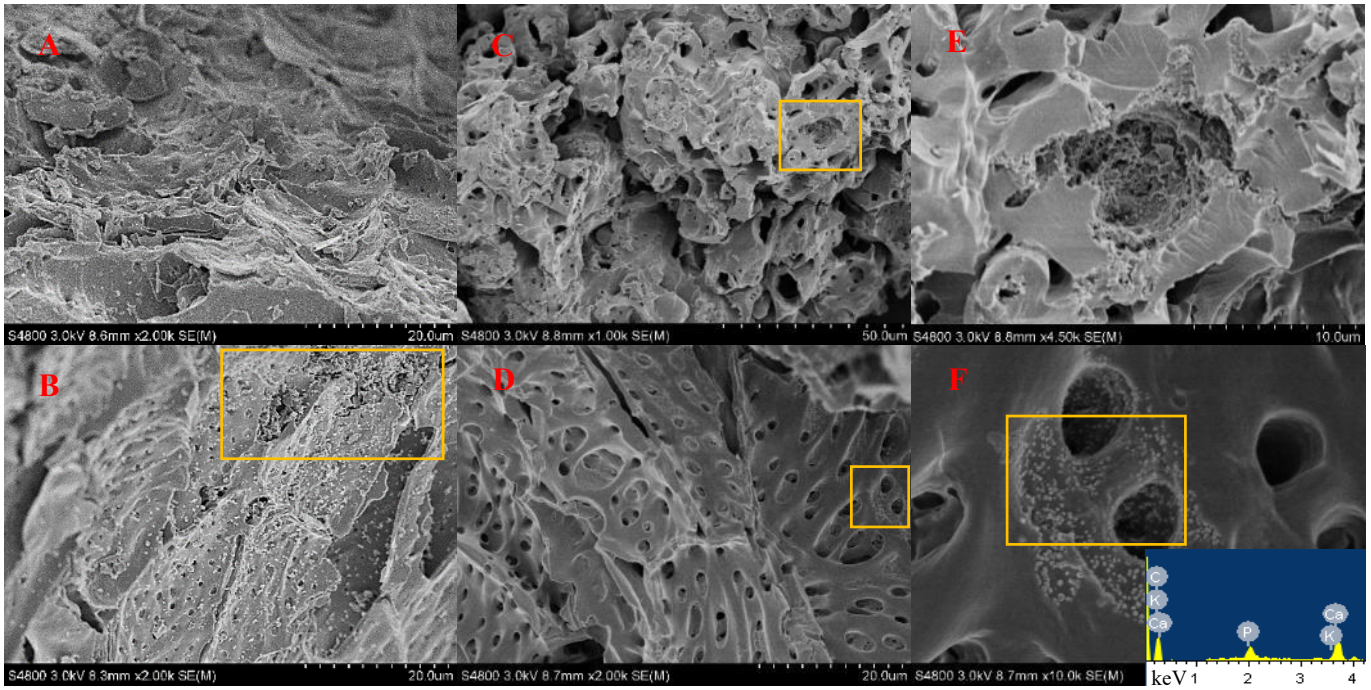

Figure S6. SEM images of bulk biochars (B-BCs) before and after the extraction for nano biochars (N-BCs). (A) B-PBC300, (B) B-PBC600, (C) R-PBC300, and (D) R-PBC600. The images in panel (E) and (F) are enlarged from the frames in panel (C) and (D), respectively. EDX spectra were collected from the frame in panel (F).

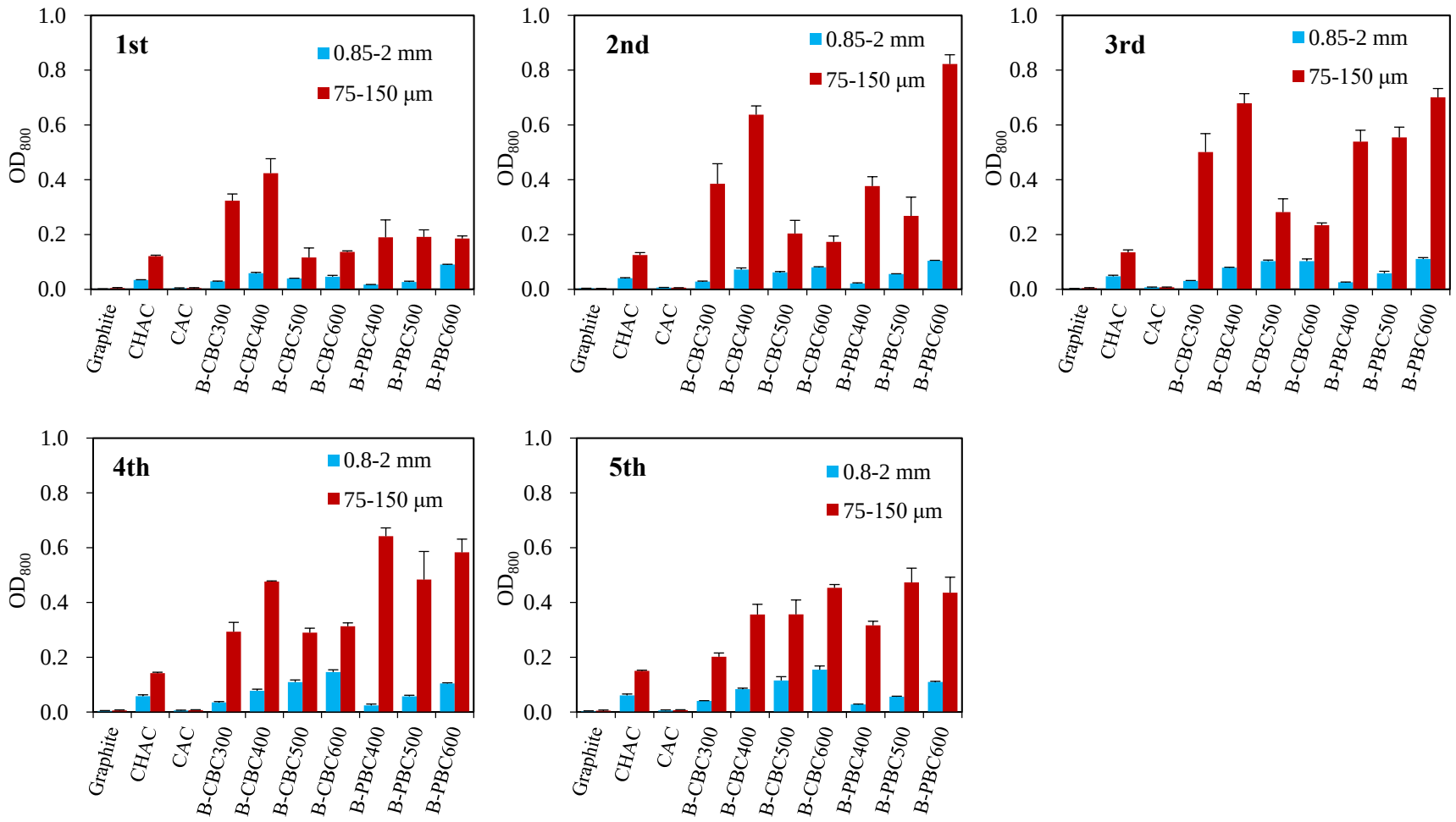

Figure S7. Release of the nanoparticles from bulk biochars (B-BCs), graphite, and activated carbon samples with different size (0.85-2 mm and 75-150 μm). B-PBC*X* and B-CBC*X* are the B-BCs from peanut shell and cotton straw, respectively, where *X* represents pyrolytic temperature. CAC and CHAC are the coal activated carbon and coconut husk activated carbon, respectively. The nano graphite and activated carbon were extracted via sonication-centrifugation treatment, similar to the procedure of N-BC extraction in the main text.

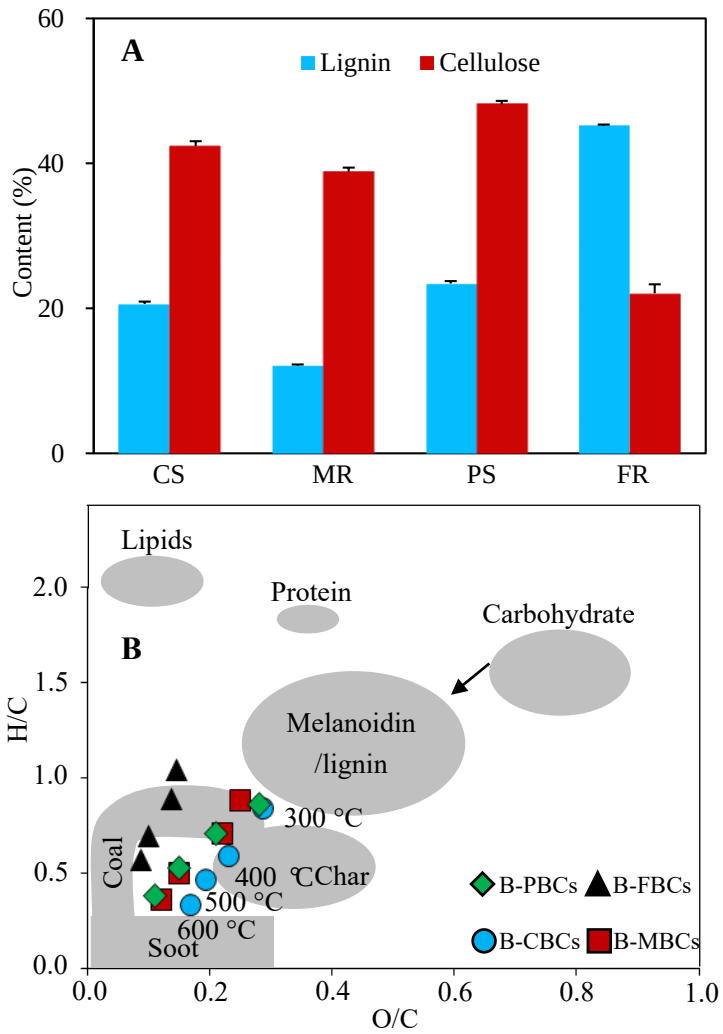

Figure S8. (A) Lignin and cellulose content of cotton straw, Chinese medicine residues, peanut shell, and furfural residues, which are referred as CS, MR, PS, and FR, respectively. (B) Van Krevelen plot of elemental ratios for bulk biochars (B-BCs) produced from CS, MR, PS, and FR (B-CBCs, B-MBCs, B-PBCs, and B-FBCs).

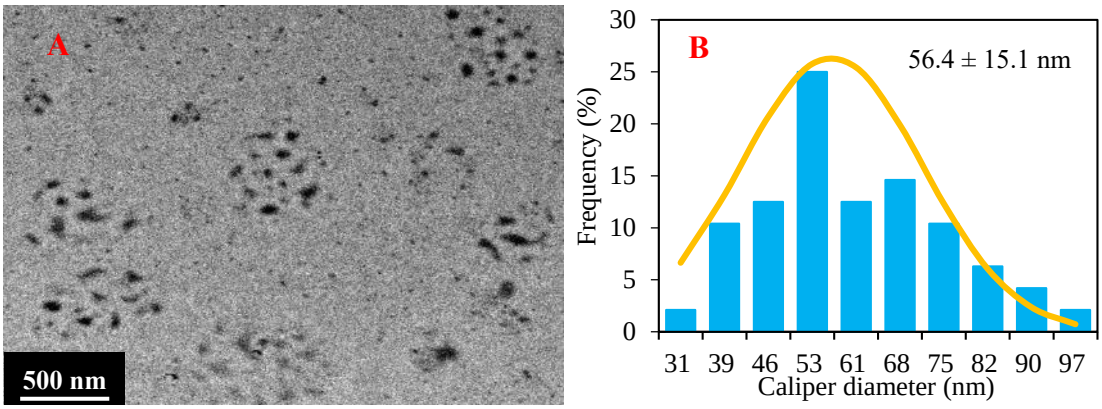

Figure S9. TEM image (A) and size distribution (B) of nano graphite (N-G).

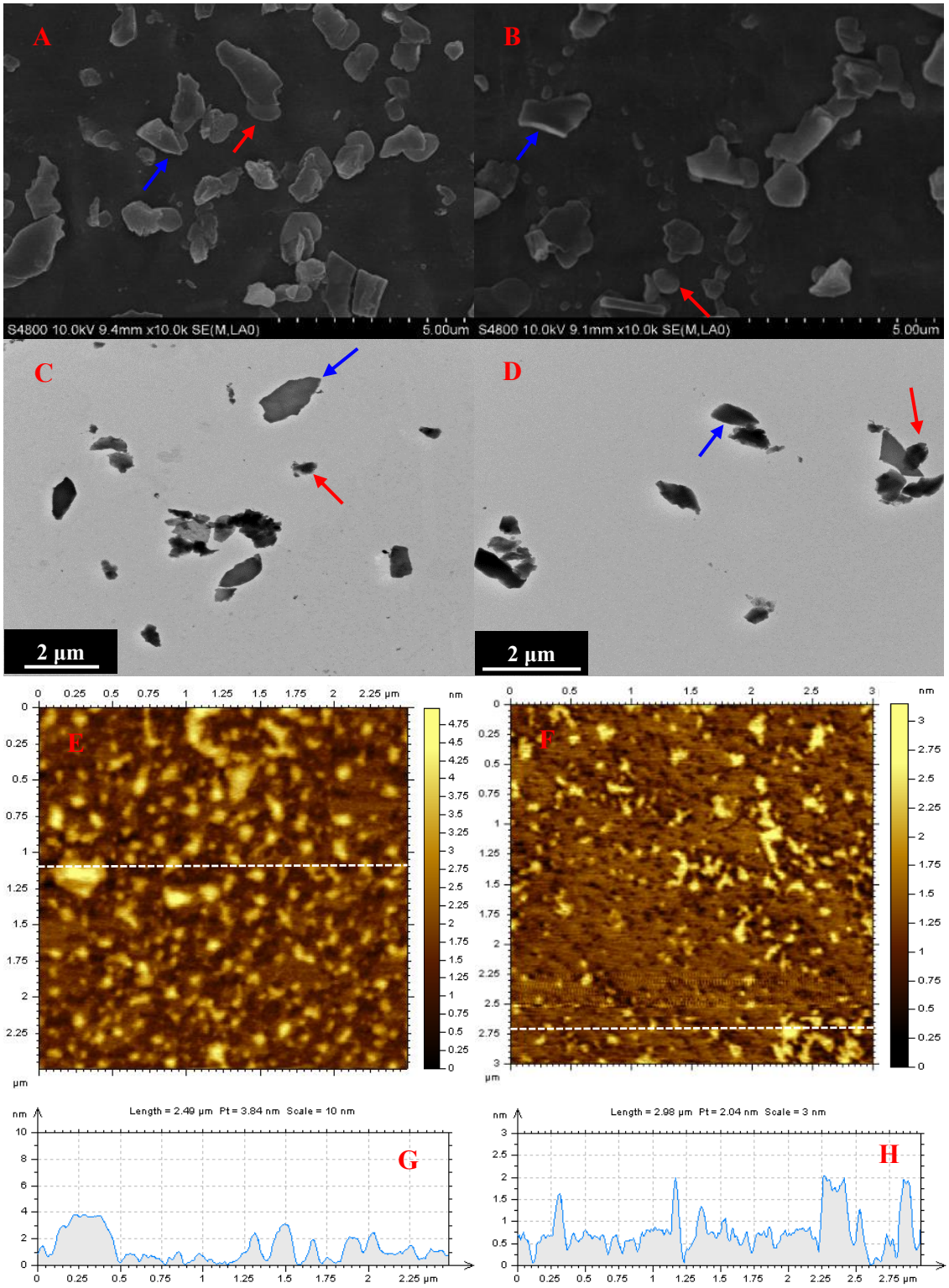

Figure S10. SEM images of (A) C-PBC300 and (B) C-PBC600. TEM images of (C) C-PBC300 and (D) C-PBC600. AFM images of (E) C-PBC300 and (F) C-PBC600. Diameter (lateral size, *x*-axis) and thickness (height profile, *y*-axis) from AFM analysis of (G) C-PBC300 and (H) C-PBC600 particles on the dotted line in panel (E) and (F), respectively.

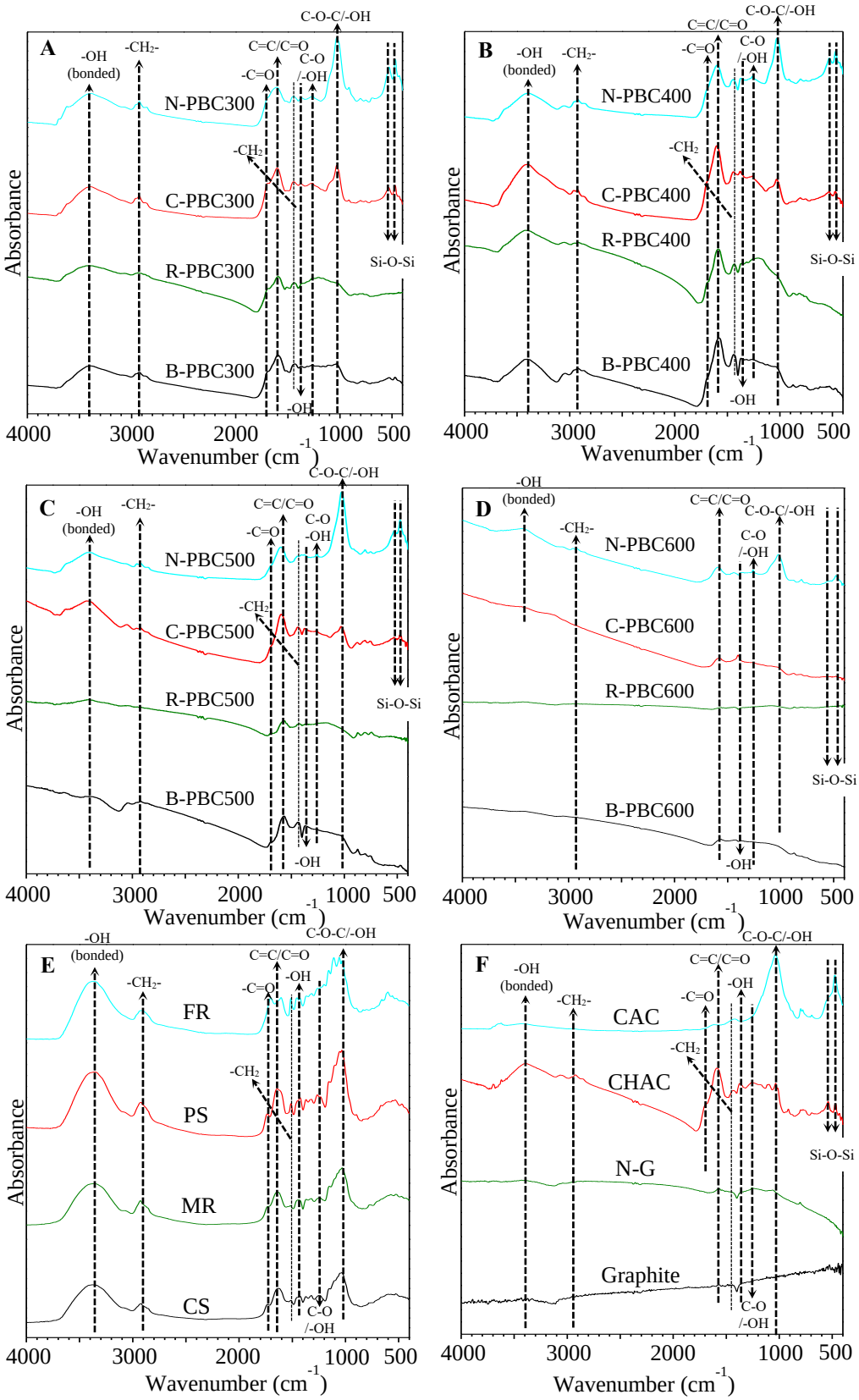

Figure S11. FTIR spectra of the biochars, feedstocks, graphite and activated carbon samples. B-PBCX, R-PBCX, C-PBCX, and N-PBCX are the bulk, residual, colloidal, and nano peanut shell-derived biochars, respectively, where X represents pyrolytic temperature. Cotton straw, Chinese medicine residues, peanut shell, and furfural residues are referred to as CS, MR, PS, and FR, respectively. CHAC, CAC, and N-G are coconut husk activated carbon, coal activated carbon, and nano graphite, respectively.

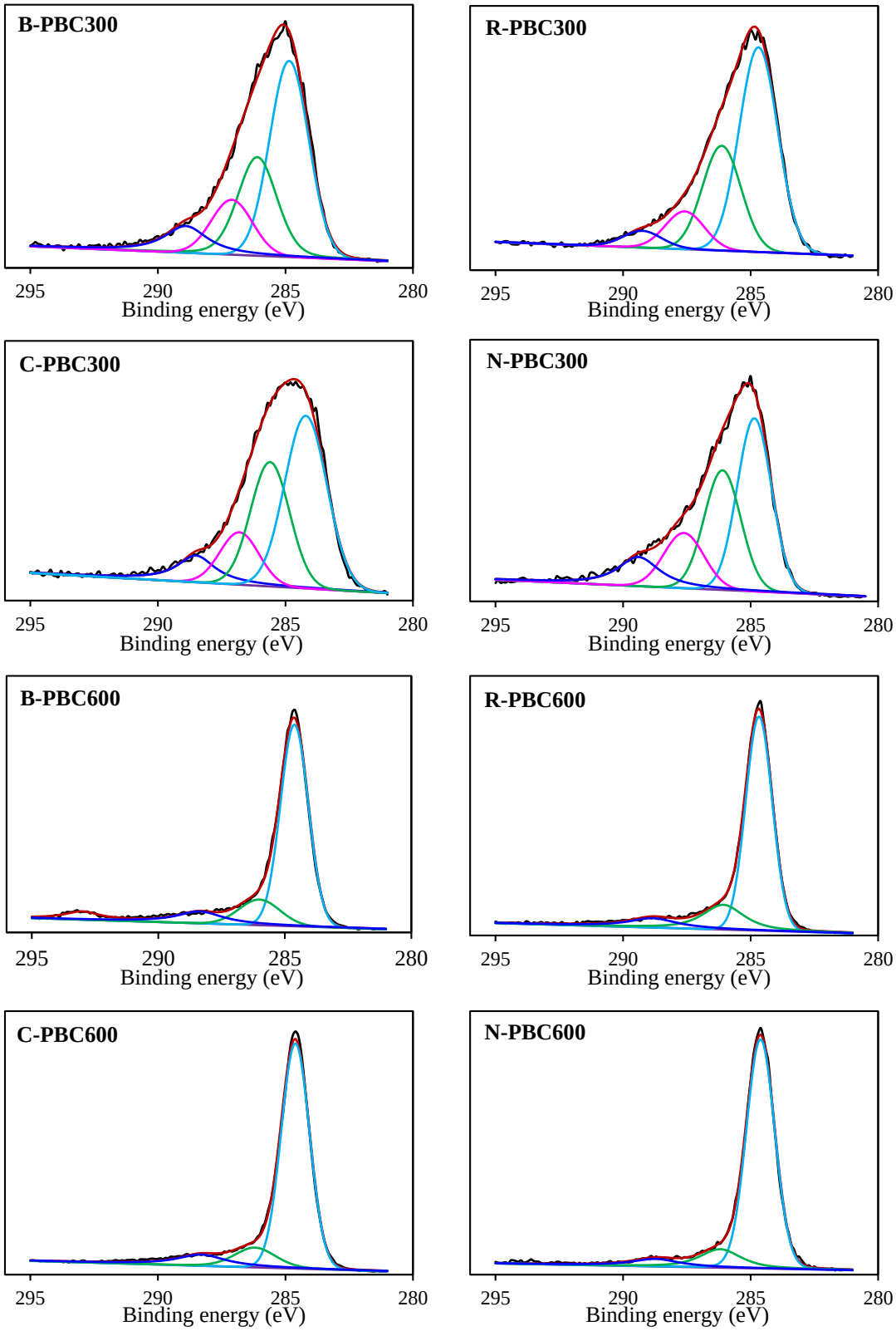

Figure S12. C1s region scan and peak fitting for the biochars by XPS. B-PBC*X*, R-PBC*X*, C-PBC*X*, and N-PBC*X* are the bulk, residual, colloidal, and nano peanut shell-derived biochars, respectively, where *X* represents pyrolytic temperature. The C1s spectra included graphitic and aromatic carbon in forms of C–C, C–H, or C=C at ~284.6 eV, C–O (phenolic hydroxyl or ether groups) at ~286.2 eV, C=O (ketone C) at ~287.0 eV, and COO (carboxylic groups) at ~289.0 eV.

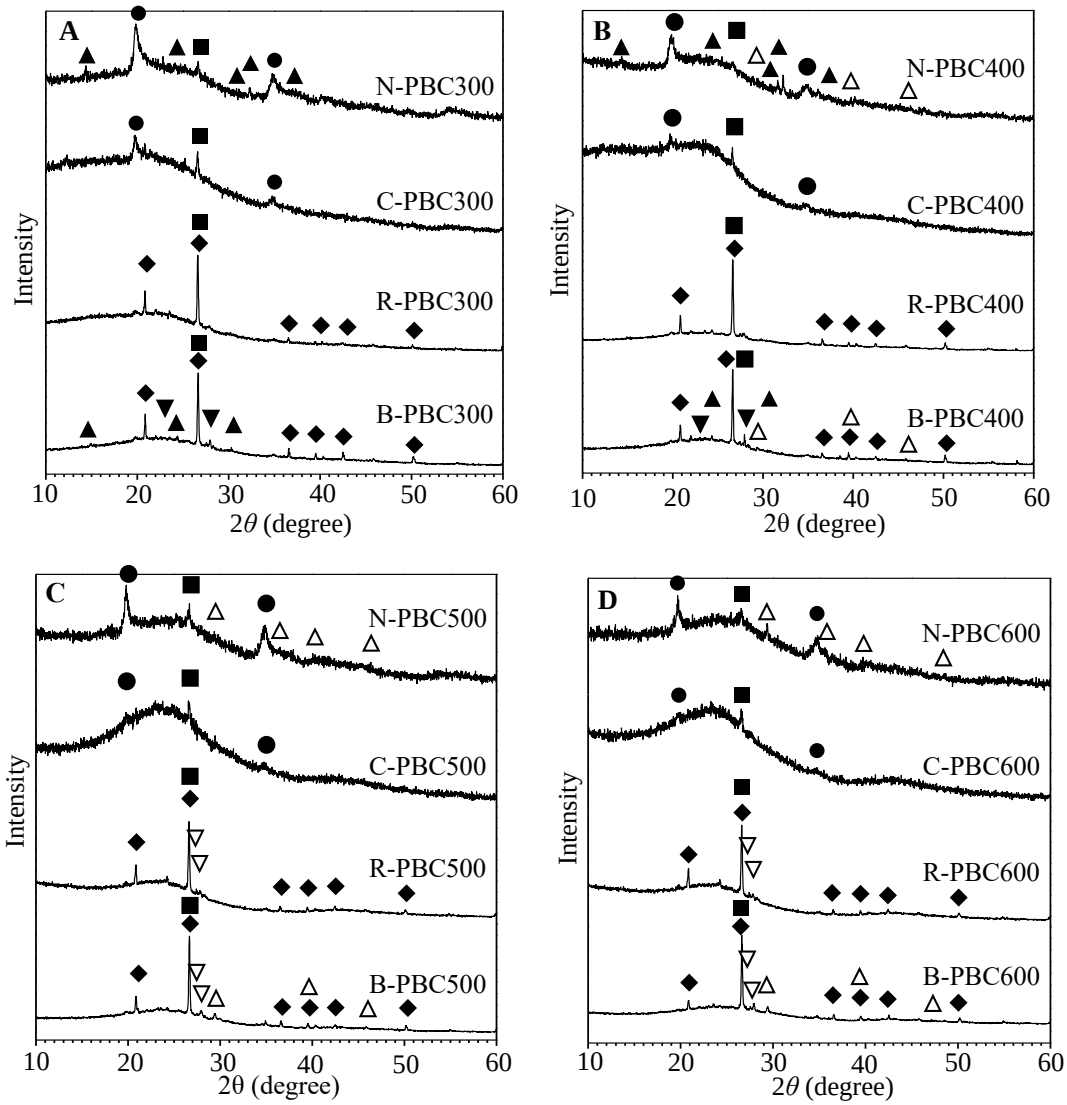

Figure S13. XRD spectra of the biochars. B-PBC*X*, R-PBC*X*, C-PBC*X*, and N-PBC*X* are the bulk, residual, colloidal, and nano peanut shell-derived biochars, respectively, where *X* represents pyrolytic temperature. The peaks of XRD were labeled as: ▲Whewellite ($CaC_2O_4 \cdot H_2O$); ▼ Calcium dihydrogen diphosphate ($CaH_2P_2O_7$); ◆ Quartz (SiO_2); ■ Graphite (C); ● Silicon dioxide (SiO_2); △ Calcite ($CaCO_3$); and ▽ Calcium Pyrophosphate ($Ca_2P_2O_7$).

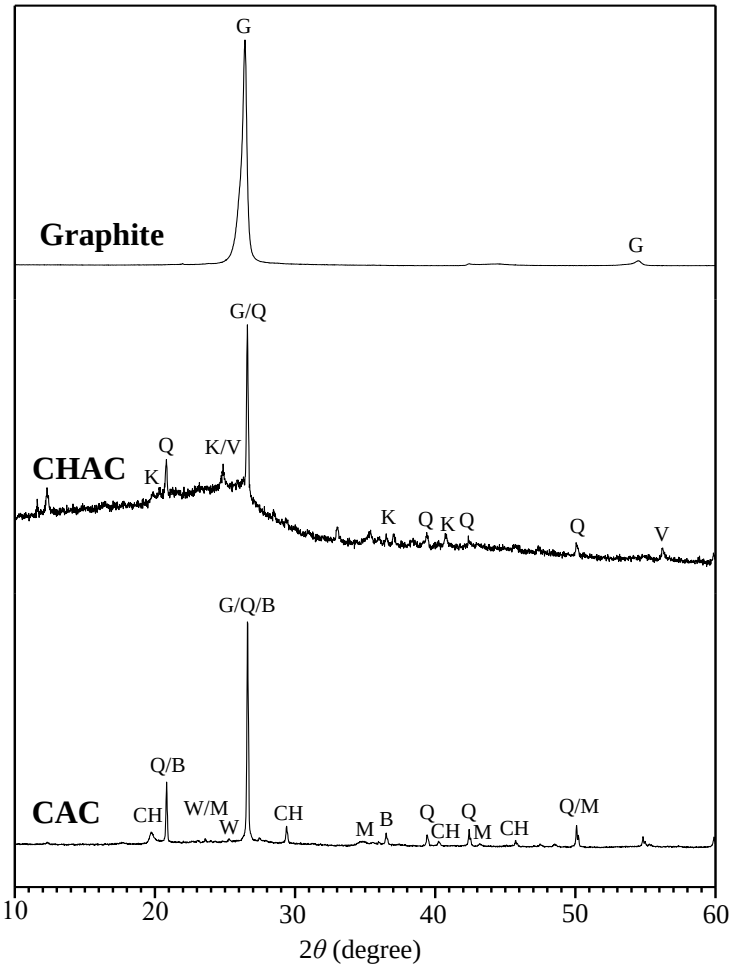

Figure S14. XRD spectra of natural graphite, coconut husk activated carbon (CHAC), and coal activated carbon (CAC). The peaks of XRD were labeled as: G: Graphite (C); V: Vaterite ($CaCO_3$); K: Kaolinite ($Al_4(OH)_8(Si_4O_{10})$); Q: Quartz (SiO_2); W: Wollastonite ($CaSiO_3$); M: Monticellite ($CaMgSiO_4$); B: Berlinite ($AlPO_4$); and CH: Chaoite (C).

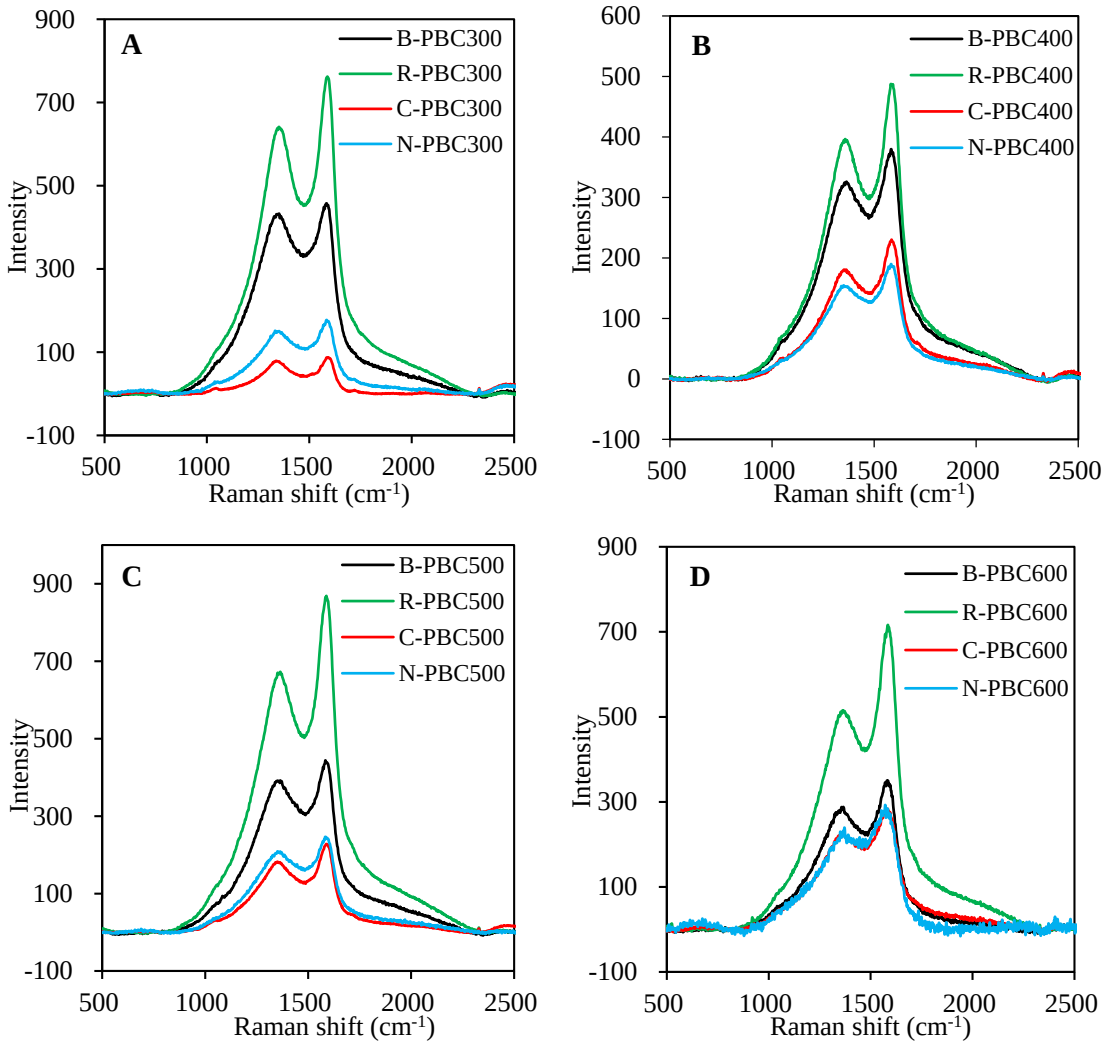

Figure S15. Raman spectra of the biochar samples. B-PBC*X*, R-PBC*X*, C-PBC*X*, and N-PBC*X* are the bulk, residual, colloidal, and nano peanut shell-derived biochars, respectively, where *X* represents pyrolytic temperatures.

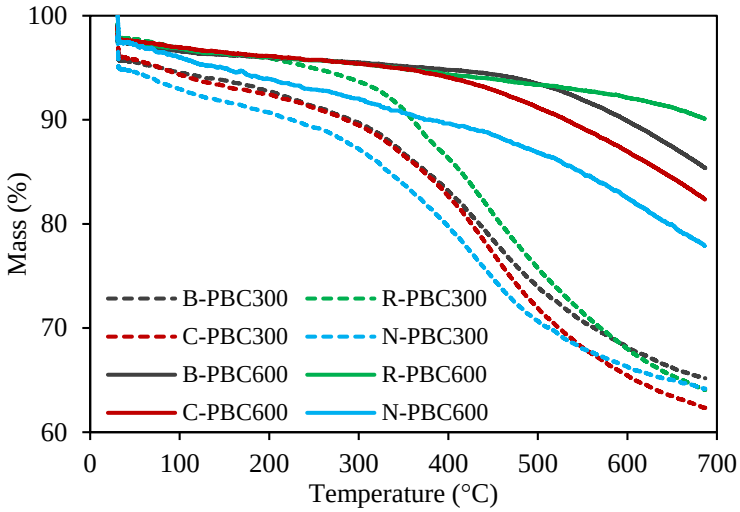

Figure S16. Thermogravimetric thermograms of different PBC fractions.

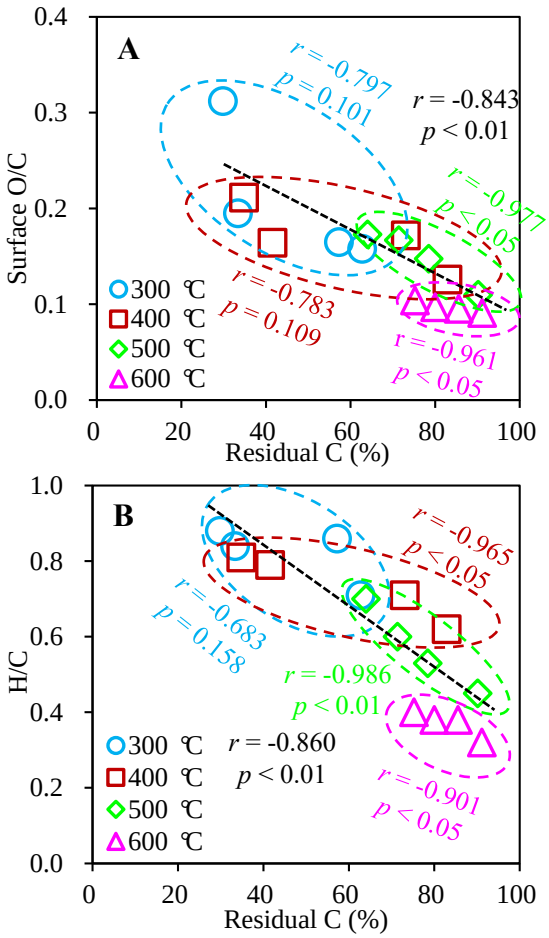

Figure S17. Correlations between the residual C content of the bulk, residual, colloidal, and nano peanut shell-derived biochars after H_2O_2 oxidation for 48 h and (A) surface O/C ratios or (B) bulk H/C ratios. Black dashed lines represent the correlations based on the data of all the biochar samples; and for a given temperature, the correlations are presented by different color dashed ellipses. The correlation coefficients (*r* and *p* value) were obtained from Pearson correlation analysis.

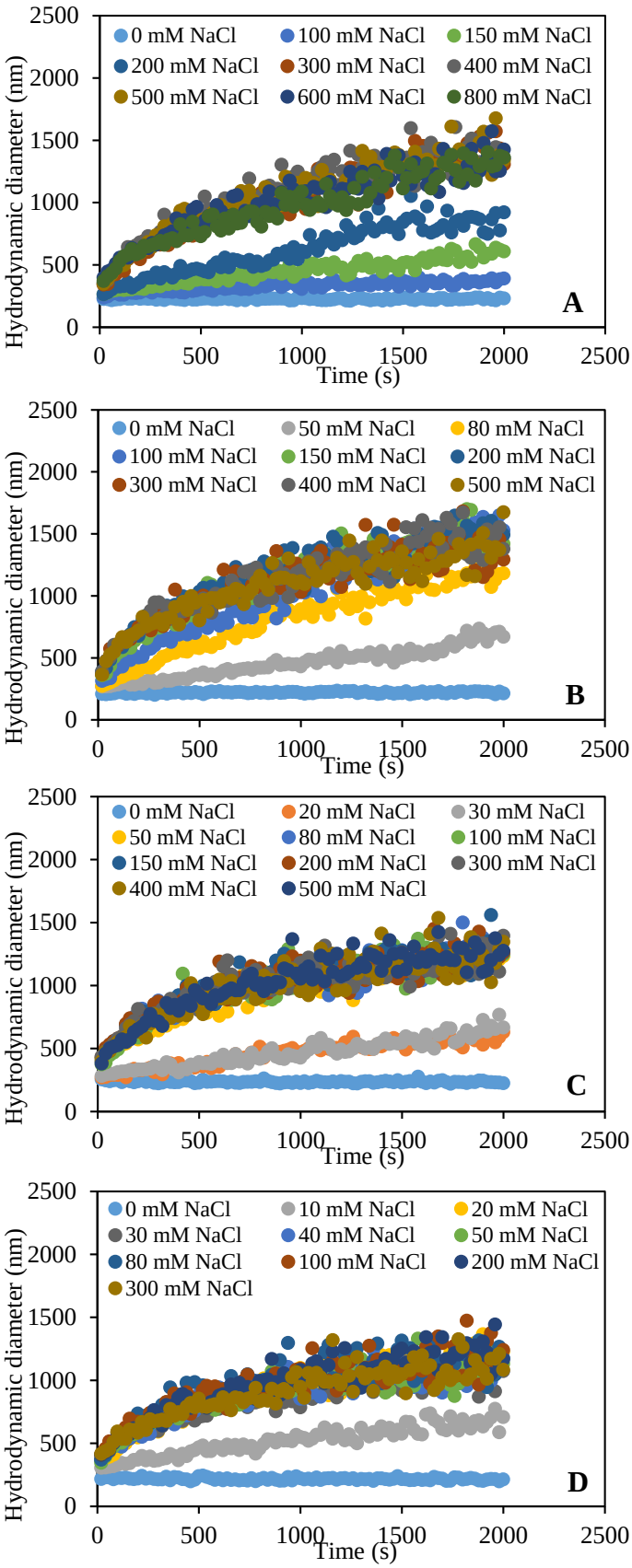

Figure S18. Hydrodynamic diameter of (A) N-PBC300, (B) N-PBC400, (C) N-PBC500, and (D) N-PBC600 at different NaCl concentrations at pH 6.8.

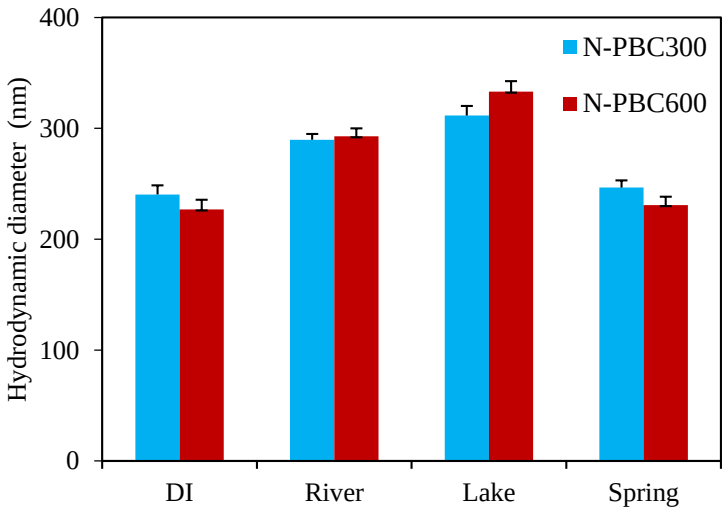

Figure S19. Hydrodynamic diameter of N-PBC300 and N-PBC600 in the natural waters at 5 days. The natural waters from Licun river, Jihongtan lake, and Laoshan spring in Qingdao, China were employed in this study.

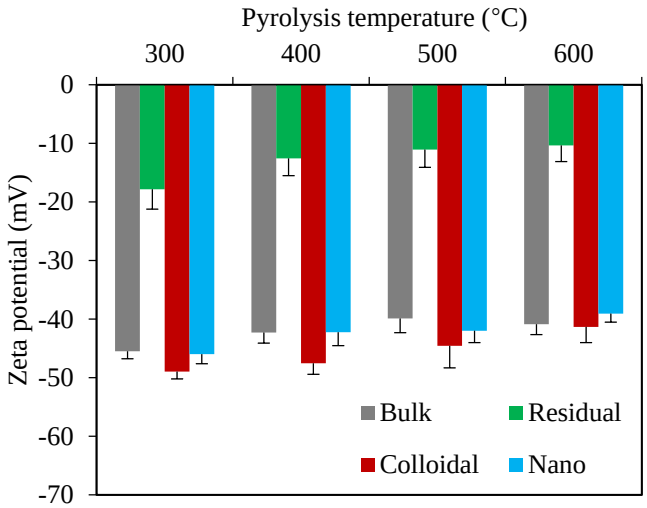

Figure S20. Zeta potentials of the bulk, residual, colloidal, and nano peanut shell-derived biochars at pH 6.8.

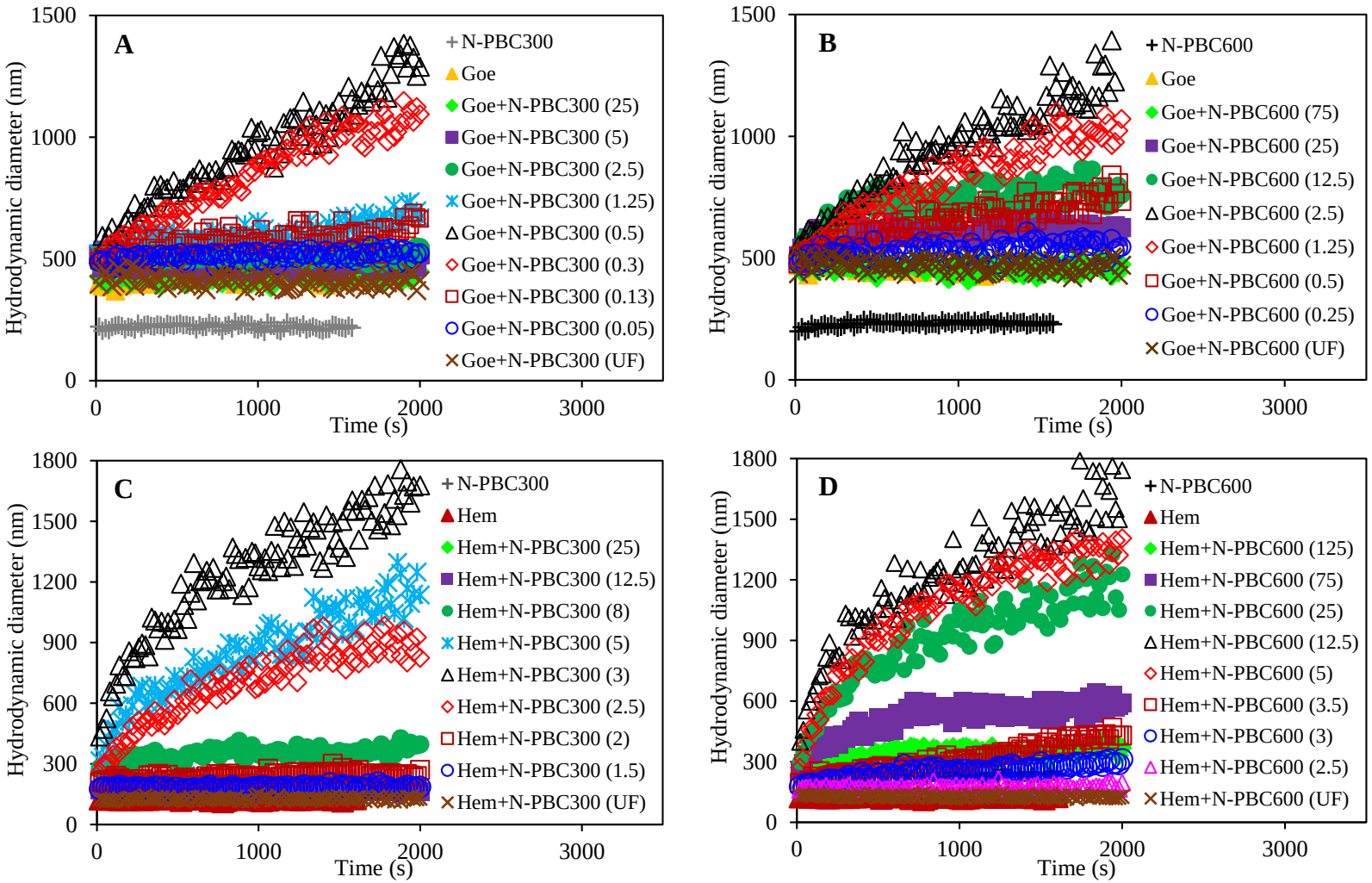

Figure S21. Heteroaggregation of Goe and Hem particles (10 mg/L) with the nano biochars (N-BCs) at various concentrations. (A) Goe+N-PBC300, (B) Goe+N-PBC600, (C) Hem+N-PBC300, and (D) Hem+N-PBC600. The dispersion of Goe and Hem particles in ultrafiltrate (UF) of the N-BC suspension was presented in all the panels.

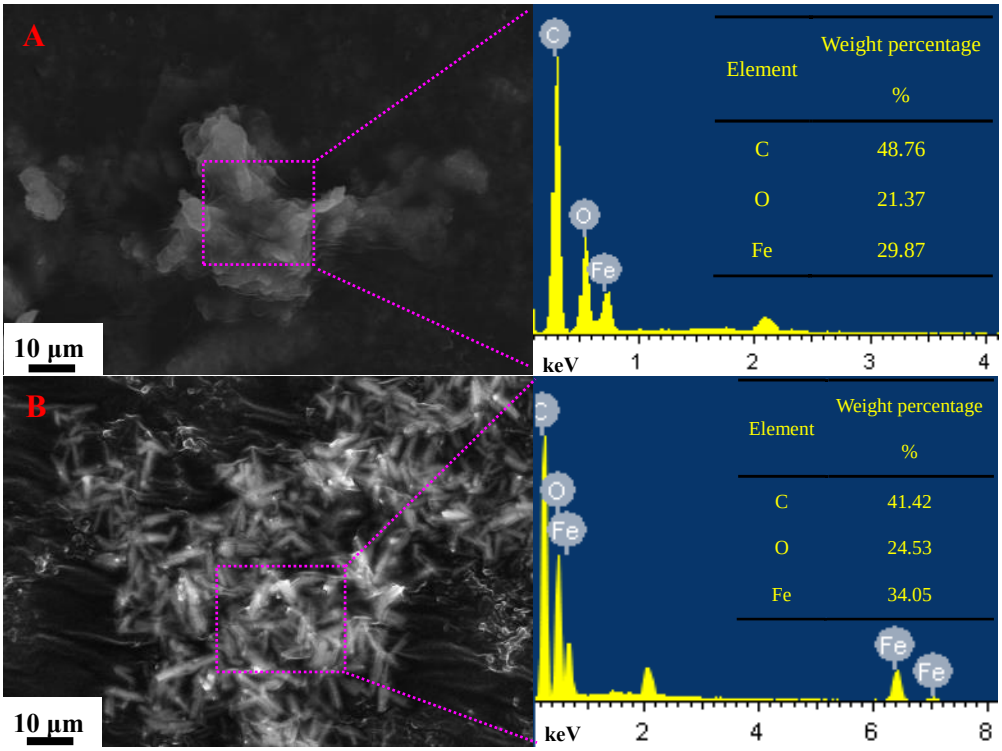

Figure S22. SEM images of the heteroaggregates of (A) Hem+N-PBC300 and (B) Goe+N-PBC300 at the peak concentration. EDX spectra of the heteroaggregates were collected from the pink frames.

REFERENCES

1. Smith C. R.; Buzan E. M.; Lee J. W. Potential Impact of Biochar Water-Extractable Substances on Environmental Sustainability. *ACS Sustain. Chem. Eng.* **2013**, *1*:118–126.

2. Spokas K. A.; Novak J. M.; Masiello C. A.; Johnson M. G.; Colosky E. C.; Ippolito J. A.; Trigo, C. Physical Disintegration of Biochar: An Overlooked Process. *Environ. Sci. Technol. Let.* **2014**, *1*:326–332.

3. Yi P.; Pignatello J. J.; Uchimiya M.; White J. C. Heteroaggregation of Cerium Oxide Nanoparticles and Nanoparticles of Pyrolyzed Biomass. *Environ. Sci. Technol.* **2015**, *49*:13294–13303.